Oxycoal combustion tests in CIUDEN

Willem Broenink, TE student
University of Twente
20-11-2015
w.a.broenink@student.utwente.nl

Preface

This report is written as part of the internship for the year 2015-2016 of the master Mechanical Engineering of the University of Twente, Enschede. Together with 3 other team members, I performed multiple tasks as contribution to the Relcom project. The paper deals with the characterization of Oxycoal combustion in the CUIDEN furnace, as well as the calibration of the heat flux meters.

Rather than starting from scratch, I was able to benefit from this on-going program at IFRF, which contributed to making this a good learning experience. I would like to thank International Flame Research Foundation for hosting my internship and allowing me to participate in the Relcom project. The same for my fellow-student Hans Geerligs and IFRF employees Giovanni Coraggio, Marco Faleni and Cristiana Gheorghe for their guidance, assistance and knowledgeable support. Last I would like to thank the CUIDEN team for allowing us to test at their 20MW_t experimental furnace, located in Ponferrada.

Summary

As part of the Relcom project, IFRF was tasked to perform full characterization of Oxycoal combustion inside a 20MW_t experimental furnace, made available by CUIDEN. The objective of this report is to describe the processing of the temperature and heat flux results obtained in the measurement campaign in CUIDEN. In addition, present a calibration procedure for both the radiative heat flux meter and total heat flux meter using the black body furnace.

In total, 3 different operation conditions are characterized, the air base mode and two different oxy combustion modes. This is done by measuring temperature and chemical composition at multiple ports and multiple insertion depths. Heat flux measurements are taken in ports along the furnace walls. In order to measure the inflame characteristics probes and data recovery equipment are used. The probes relevant to the measurement of the total heat flux, radiative heat flux and temperature are the Total heat flux meter, ellipsoidal radiometer and the suction pyrometer respectively. The data recovery equipment consists of the 34970A data logger and corresponding software called *free Benchlink datalogger software* which are able to measure the different signals from the probes.

The total heat flux meter and ellipsoidal radiometer require calibration in order to convert the signals into the corresponding heat fluxes. This is done using a black body furnace located in the IFRF workplace. The calibration is performed both before and after the measurement campaign and the results averaged. Together with processing of the data the performances and error estimations for the heat flux probes were obtained.

After processing of the obtained data from the measurement campaign results for the heat flux and temperature are obtained. Results for the heat flux are presented as the heat flux values and corresponding errors versus the exhaust path. Temperature results are presented as temperature values versus the boiler axis distance.

It can be concluded that the furnace was able to maintain the Temperature and heat extraction when introducing Oxycoal combustion. Therefore avoiding the formation of NO_x and the introduction of thermal strain of the furnace walls and burner.

Table of content

Introduction

In today's energy production industry, coal is one of the main sources of fossil fuels. It is expected that for at least some decades the implementation of coal as fuel will not reduce. To decrease the impact of climate change, it is therefore required to reduce the CO2 emission's related to the combustion of coal. The eventual goal being near-zero emission's through carbon capture and storage (CCS) techniques. Oxycoal combustion is one such technique, where coal is fired with oxygen instead of air. The flue gasses produced largely consist of CO2 and water vapor so that CO2 purification is readily achieved.

The RELCOM project is designed to acquire a greater understanding of Oxycoal combustion. This is done through a series of applied research, development and demonstration activities. Both experimental studies and modelling work contribute to designing full-scale Oxycoal combustion plants with greater confidence as well as providing improved assessment of the commercial risks and opportunities. As one of the participating partners for the RELCOM project, IFRF was tasked to perform a full characterization of the inflame conditions for Oxycoal combustion. Characterization included the measurements of temperature and chemical compositions, as well as heat fluxes in different spatial points inside a furnace. An example of the implementation of this data being the verification of results found by modelling of Oxycoal combustion.

For the RELCOM project an experimental combustion plant was made available by 'The Technology Development Centre for CO2 Capture' (CIUDEN), located in Ponferrada (Spain). It is designed for the combustion of pulverized coal with outputs up to 20 MW_t The combustion plant is also equipped with a flue gas recirculation and cleaning system and oxidant preparation system to test Oxy-combustion [2]. A picture of the experimental combustion plant is shown on the front page.

The objective of this report is to describe the processing of the temperature and heat flux results obtained in the measurement campaign in CUIDEN. In addition, present calibration procedure for both the radiative heat flux meter and total heat flux meter using the black body furnace. Subjects included in this report are: measurement campaign work plan, measurement equipment and data recovery equipment, calibration of the heat flux meters, results, conclusions and discussion.

1 Measurement campaign

IFRF was tasked to perform in-flame measurements in the CUIDEN rig during Oxycoal and conventional air/coal combustion tests. Measurements for temperature and chemical composition were done for different spatial points inside the furnace. Heat fluxes were measured in different spatial points along the wall of the furnace. Subjects included in this chapter are the different operation conditions of the furnace, the work plan for characterization of the inflame conditions and the experimental setup of the measurement equipment.

1.1 Operation conditions

In total, three different steady state flame modes were characterized. Characterization of each mode took 9 to 14 hours to complete. The combustion modes are shown in Table 1. An Air base case was introduced to function as reference for the results found in the Oxy mode cases. Differences in the Oxy mode cases included the points of injection of oxygen and overall oxygen concentration. However, due to confidentiality these will not be discussed in this report.

Mode	Test Code	Explanation
Air-combustion mode	S2-A1	Air base case
Oxy-combustion mode, premixed	S2-01	Oxy mode base case
Oxy-combustion mode	S2-017	Oxy mode with increased oxygen concentration

Table 1, list of all combustion modes

As mentioned in the introduction, the combustion plant is equipped with flue gas recirculation in order to obtain similar inflame temperatures to the Air-combustion case. If not used, Oxycoal combustion would result in temperatures higher than the maximum allowable temperature of the furnace, leading to the formation of NO_x (nitrogen oxide) and thermal strain of the furnace walls and burner. By recirculation of the flue gas with additional cooling the temperature of the flame can be regulated due to additional energy absorption capacity of the flue gas.

1.2 Work plan

To perform the in-flame measurements, probes are inserted into the furnace with varying insertion depths.
shows a schematic overview of the furnace and specifies the location of the different ports and insertion depths. Please note that the insertion depths for Temperature and chemical species vary for the different combustion modes. Associated with
is Table 2, showing the measurements performed in the different ports for the different combustion modes.

Test Code	Level position	Port number	Temperature	Chemical species	Radiative heat flux	Total heat flux
REL-BIT-S1-01bis	2	6	X	X	-	X
	2	7	X	X	-	X
	3	18	X	X	X	X
	5	32	X	-	X	X
	5	36	-	-	-	-
	6	40	X	X	-	-

REL-BIT-S1-A1	2	6	X	X	X	X
	2	7	X	X	X	X
	3	18	-	-	-	-
	5	32	X	X	X	X
	5	36	-	-	-	-
	6	40	-	-	-	-
REL-BIT-S1-017	2	6	X	X	X	X
	2	7	X	X	X	X
	3	18	X	X	X	X
	5	32	X	-	X	X
	5	36	X	-	-	-
	6	40	X	X	-	-

Table 2, list of all measurement ports for the different probes, for all combustion modes

1.3 Setup measurement equipment

In order to measure the inflame characteristics of the different combustion modes the following setup will be used, also shown in Figure 1. Associated with Figure 1 is Table 3 listing all the measuring devices corresponding to the numbers shown in Figure 1.

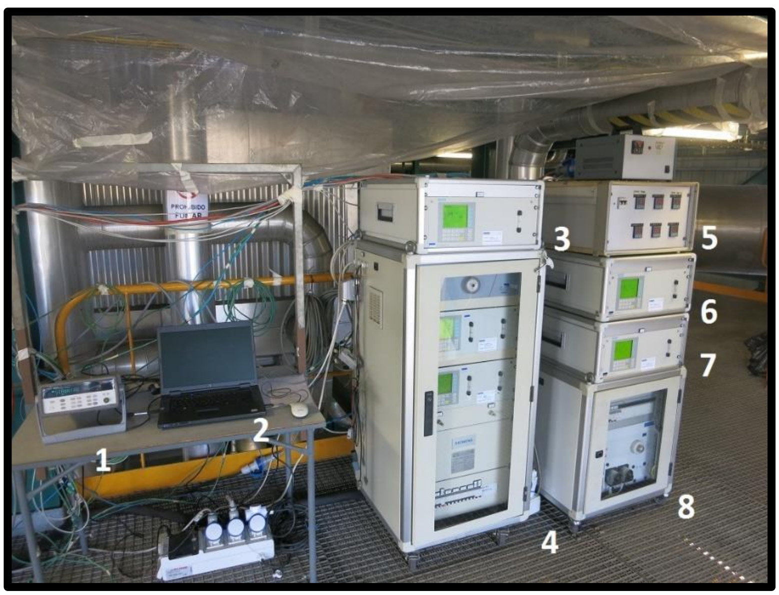

Figure 1, measuring devices setup

No.	*Part type*
1	Datalogger, converts all the incoming signals in voltages.
2	Laptop, uses an external datalogger to receive information from the Siemens analyzers and thermocouples
3	Siemens Ultramat NDIR, CO concentration

4	Siemens Ultramat/Oxymat 6 NDIR and paramagnetic oxygen analyser
5	Regulators for temperature in the sample line and filter
6	Siemens Ultramat NDIR, CO2 concentration
7	Siemens Oxymat, O2 concentration
8	Suction pump including a dryer, connected to the sampling probe by heated lines

Table 3, list of all measurement devices including the corresponding numbers

2 Probes and data recovery equipment

Measurements of the furnace characteristics are performed using probes [3]. The probe types used by IFRF consist of long tubes with water jackets for cooling. This allows for the use inside furnaces at varying spatial coordinates along the direction of insertion. The mechanics used to evaluate the furnace characteristics are uniquely related to the different probe types. In total 4 different probe types are used for the measurements performed in CIUDEN, listed in Table 4.

Probe type	Physical quantity
Suction pyrometer	Inflame gas temperature
Ellipsoidal radiometer	Radiative heat flux
Total heat flux meter	Total heat flux
Sampling probe and analyser	Gas chemical composition

Table 4, list of different probe types used and the corresponding physical quantity measured

In this report only the first 3 probe types will be discussed, since these are used for measurement of the temperature and heat fluxes. Subjects included in this chapter are a description, setup, performance and operation for each of the different probe types. More information about the sampling probe can be found in [4]. Figure 2 shows an example of the probes during operation. In addition, information about the data recovery equipment will be provided.

Figure 2, probes during operation in CUIDEN

2.1 IFRF suction pyrometer

As mentioned before, the Suction pyrometer is used to obtain a more or less accurate measurement of the inflame gas temperature. A schematic overview of the Suction pyrometer probe is provided in Figure 3. Elements included in the suction pyrometer are an S-type thermocouple, a sintered alumina sheath for protection against chemical attack and 2 ceramic shields to protect against external radiation. The combustion gas is drawn through an opening in the outer ceramic shield with a high suction rate and exchanges heat with the thermocouple. Hence the thermocouple will reach temperatures close to the temperature of the gases without the need for significant corrections [1].

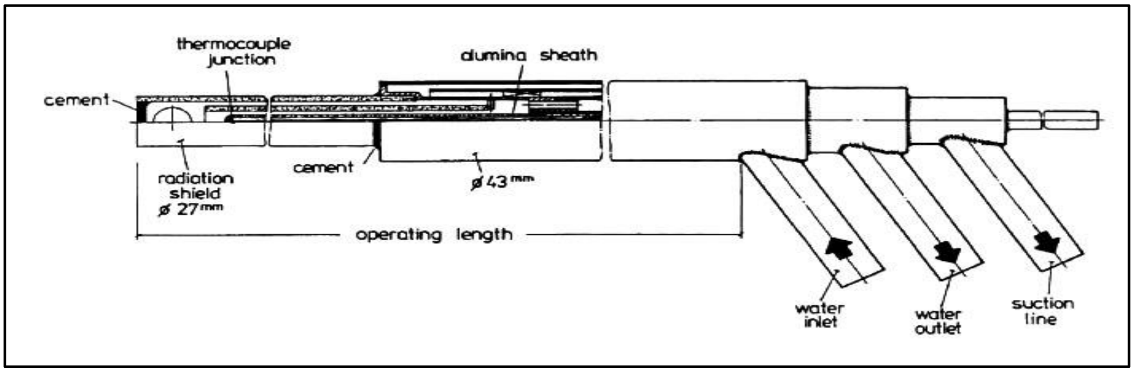

Figure 3, schematic overview of the suction pyrometer [5]

2.1.1 Suction pyrometer setup

In order to operate the Suction pyrometer three auxiliaries are required. The cooling water line for the water jacket, a vacuum pump for the gases and a voltmeter for the S-type thermocouple. To attach both the waterline and the Suction pump, the Suction pyrometer contains 3 attachment points which are shown in Figure 3. Placement of the different connections is as follows: the Suction pump is connected to the outer tube. The two innermost tubes are used for the cooling water. To acquire the most effective cooling a counter flow is introduced by connecting the cooling water inlet to the inner tube and the outlet to the middle tube. The thermocouple is placed inside the Suction pyrometer in the positioning duct. The IFRF Suction pyrometer uses two concentric ceramic shields and one alumina sheath, the setup is shown in **Error! Reference source not found.**. To minimise clogging of the shields, the opening in the ceramic shield is positioned in opposite/perpendicular direction to the gas flow inside the furnace.

No.	*Part type*
1	Alumina sheath
2	Inner shield
3	Outer shield

2.1.2 Suction pyrometer performance

Possible error sources of the pyrometer due to instrumentation can be listed as: gas velocity, conduction of the thermocouple wires, radiation, intrinsic error of the thermocouple and voltmeter. IFRF performed analysis of the total sum of the different error types with the use of theoretical background. Results are shown in Figure 6. It can be seen that the total error due to instrumentation is 8.6°*C*. From the conservative point of view it is chosen to use 10°*C* as standard value.

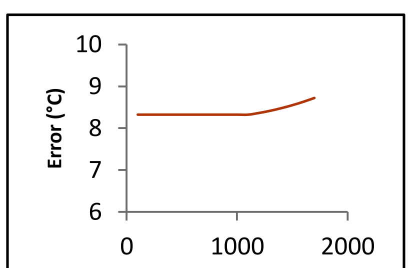

Figure 4, error behavior pyrometer [1]

During combustion, values for Temperature are ever changing and (as will later be explained in data recovery) the value reported for each measurement point is the average over a time interval. Calculation of the standard deviation over the same time interval has been assumed as statistical error. This quantity contributes to overall uncertainty of the probe and also provides insight in fluctuations of the measured physical quantity in every point. The total error is given as 2-1. The typical response time of the Suction pyrometer is in the order of 1 minute.

$$\Delta T_{total} = \sqrt[2]{\Delta T_{instrumentation}{}^{2} + \sigma_{timeinterval}(T)^{2}} \tag{2-1}$$

The position reported in the results contains a position error. This positioning error is mainly due to inability to control the probe without errors in an industrial environment. Examples are tipping of the probe after insertion, causing deviations from the insertion line up to 50mm. As well as the use of measuring tape to measure the insertion depth using varying reference points along the walls of the furnace. Therefore it is assumed that the accuracy of the position is +-15 mm along horizontal direction and +-50mm in vertical direction. It is important to note that the temperature values relative to a measurement point are not punctual, but an average of the values of a region inside the furnace centered in the measurement point. IFRF experimental experience makes it safe to assume a radius of 2.5 cm [1].

2.1.3 Suction pyrometer operation

Before starting tests, make sure that the water is circulating into the probe. Then wait a few extra minutes to avoid air bubbles remaining inside the probe. Typical water pressures are between 3-5 bars at the cooling water inlet [5]. Since the probes will be operated far from the pump, pressure drops in the pipeline and connections might occur. This is why all of the probes contain a bar meter connected to the cooling water inlet. Insufficient cooling can lead to bending or destruction of the probe, an example of bending is shown in Figure 5 (please note this is also the case for the other probes).

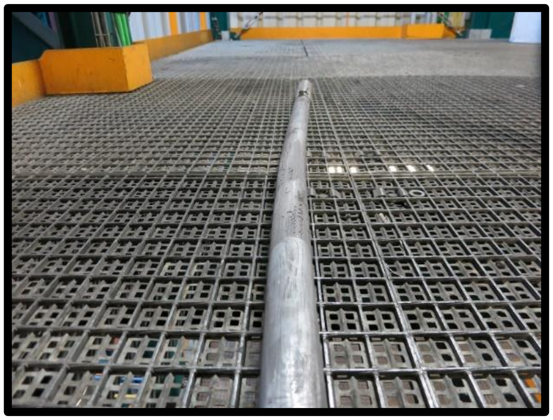

Figure 5, picture of the suction pyrometer after thermal deformation

During measurements, the shields can break or clog because of ash. To ensure reliable results it is therefore required to extract the probe and replace or clean the shields. In addition, the integrity of the shield has to be controlled regularly during operations. Slow response times with steady temperature output could indicate ceramic shield failure. In addition it is also possible for the thermocouple to break on impact. When this happens it is required to remove and replace the thermocouple. Both occurrences are shown in Figure 6.

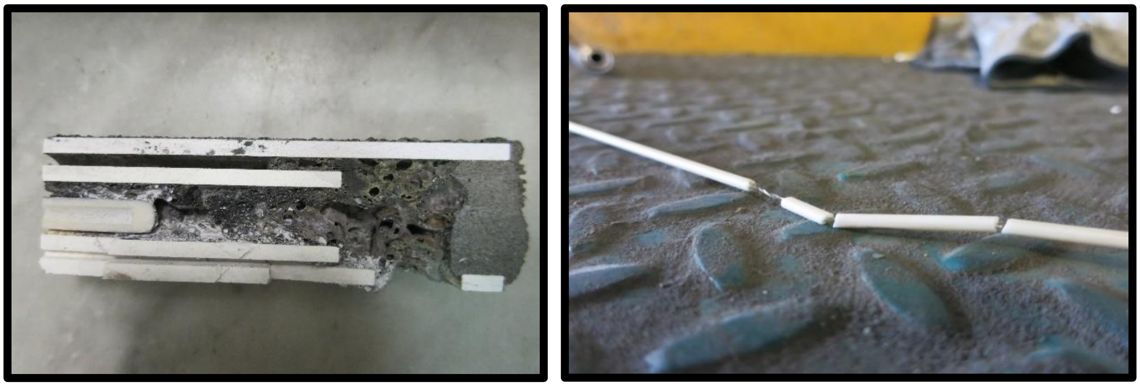

Figure 6, cross section of the ceramic shields showing ash plugging (left), broken thermocouple (right)

2.2 IFRF Ellipsoidal radiometer

The Ellipsoidal radiometer is used to measure the total radiative heat flux coming from the medium located in front of its tip. The main application is to investigate the magnitude and distribution of radiative heat fluxes hitting the walls of the furnace. A schematic overview of the Ellipsoidal radiometer is provided in Figure 7.

The ellipsoidal radiometer consists of a hollow ellipsoidal cavity with a mounted orifice at one side and a mounted thermophile at the other. The cavity has the optical property of focusing all radiation entering the orifice onto the sensitive surface element of the thermophile. To minimize radiation losses due absorption, the ellipsoidal surface is covered with a gold film. The ellipsoidal cavity is divided into two parts separated by a special glass. This will ensure that the inner part is isolated from the outside environment to avoid contamination from the material of the furnace and prevent convective heat transfer. In the outer part cavity nitrogen injection is used to purge contaminations and reduce the infiltration of dusts. The thermophile is a heat flow plug of stainless steel with two thermocouple junctions at each end, which produces an e.m.f. proportional to the energy absorbed by the pellet. The maximum signal output of the thermophile is up to 15mV [1].

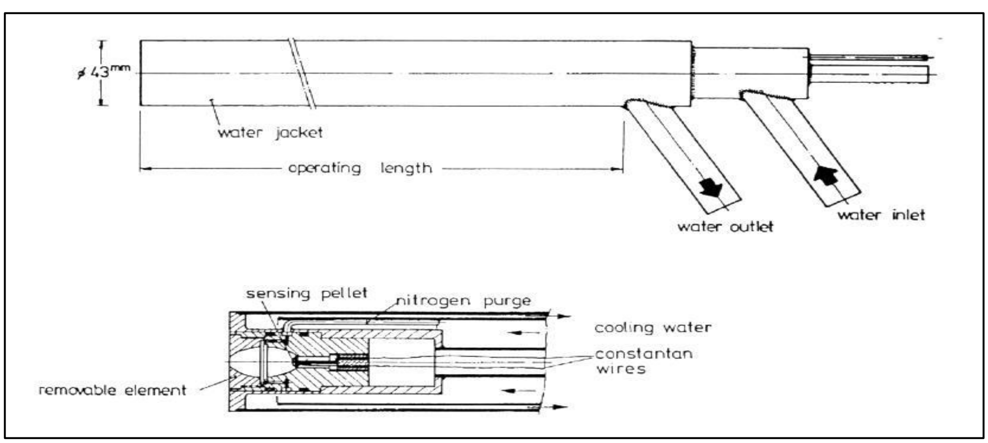

Figure 7, schematic overview of the ellipsoidal radiometer [1]

In order to ensure good performance it is necessary to calibrate the probe. This is because calibration can be used to compensate for any effects which might reduce or enhance the radiative heat flow to the thermophile. For example, despite the nitrogen injection, few solid/liquid particles might still settle on the ellipsoidal surface. Leading to increased selectivity and losses in efficiency. In advance, due to mechanical shock or thermal heating the positioning of the pellet might change or a differing area of the orifice, leading to more or less heat transfer to the receiving thermophile [6].

2.2.1 Ellipsoidal radiometer setup

In order to operate the Ellipsoidal radiometer 3 auxiliaries are required. The cooling water line for the water jacket, the nitrogen line to purge the sensor cavity and a voltmeter. To attach both the waterline and the nitrogen line the Ellipsoidal radiometer contains 3 attachment points which are shown in Figure 7, which are located at the end of the probe. Similar to the Suction pyrometer optimal cooling is achieved by connecting the water inlet to the inner tube and outlet to outer tube.

2.2.2 Ellipsoidal radiometer operation

Before using the ellipsoidal radiometer it is required to wait about 2 minutes for the radiometer to reach an equilibrium state. This can be verified when the output signal will remain constant over time. Nitrogen flow rate are typically between 0.8 and 1.2 Nm^3/h, depending on the amount of sooth present in the furnace or the pressure of the outside environment [6].

2.3 IFRF Conductivity plug-type heat flow meter (Total heat flux meter)

This probe measures the total heat flow, the sum of convection, radiation and conduction, absorbed from the combusting flow to its front surface. A schematic overview of the Total heat flux meter is provided in Figure 10.

The working principle is based on the measurement of the temperature gradient inside a solid cylinder with known thermal conductivity coefficient, by using two K-type thermocouples inserted along the axial line with known separation distance. The Total heat flux meter consists of a central stainless steel plug, mounted on the tip of the probe. The plug has a hot side subjected to the furnace and a rear end which is water cooled. Two guard rings of the same material as the plug with thin air layers in between are used to insulate the plug. Two K-type thermocouples are inserted along the axial line with a known separation distance. Please note that instead of using wires connected to the hot/cold junction inside the thermophile of the Ellipsoidal radiometer, the Total heat flux meter uses 2 thermocouples [1].

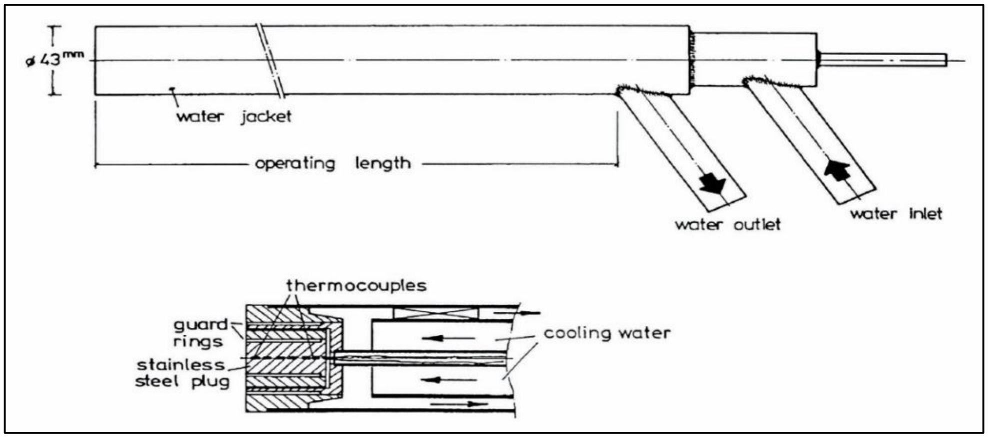

Figure 8, schematic overview of the total heat flux meter [1]

The insulation is used to provide a one dimensional heat flow along the axial line of the cylinder from the hot to the cold side. Then the conductive heat flux can be formulated as 2-2.

$$\dot{Q}_{conduction} = -\lambda \frac{dT}{dx}, \qquad [W/m^2]$$

2-2

With the thermal conductivity λ as physical property of the material type (also function of T). When defining 2 points with different spatial coordinates along the axial line of the plug, the following relation for the heat flow can be derived as 2-3.

$$\dot{Q}_{conduction} = \dot{Q}_{total} = -A\lambda_m \frac{T_2 - T_1}{x_2 - x_1}, with\ \lambda_m = \frac{\int_{T_1}^{T_2} \lambda dT}{T_2 - T_1}$$

2-3

$\dot{Q}_{cond}$	= conductive heat flux
λ_m	= mean thermal conductivity
T_1	= Temperature thermocouple 1
T_2	= Temperature thermocouple 2
A	= area

The above formulation can only be applied in the most ideal case [3]. In practice part of the heat is lost to the side walls. In addition, the thermal conductivity is hard to predict. Hence calibration is applied to ensure reliable results. This is done by determining the proportionality constant, describing the relation between the conductive heat flow through the plug and the temperature difference between the thermocouples in steady state [1].

2.3.1 **Total heat flux meter setup**

The auxiliaries needed for the Total heat flux meter are similar to the Ellipsoidal radiometer minus the need for nitrogen injection. An overview of the connection tubes and thermocouple wires is given in Figure 10Figure 10, schematic overview of the total heat flux meter [1].

2.3.2 **Total heat flux meter operation and maintenance.**

During measurements, the sooth inside will lead to contaminations in the insulation channels. To avoid the additional error cause by these contaminations, the probe head is decontaminated before every measurement point by the use of a steel brush and compressed air [7].

2.4 Position of the heat flux probes

During measurement campaigns at the 20MW CIUDEN facility, some instances occurred where the measured total heat flux was lower than the radiative heat flux. Under normal circumstances this should not occur, therefore the situation is analyzed by IFRF.

Standard procedure for the heat flux probes is to position them in alignment with the boiler wall. However, as visible in Figure 9 deposition on the walls of the furnace can obscure the field of view of the probes. The THF meter has a bigger surface to capture the radiation of the flame, its field of view will be affected more by the ash deposition on the walls. This results in lower measurements for the total heat flux. Secondly, the area just in front of the probe is possibly stationary because it is trapped between ash decompositions. Cooled by the probe, it could form a cold area in front of the probe. This pocket of colder gas lowers the convection received by the total heat flux meter. This led IFRF to adjust the position of the probe. By placing the probes further into the furnace, these problems are averted. During the CIUDEN campaign probes are inserted 5-10 cm further into the furnace resolving the problems. In big furnaces the slight difference in position is not expected to alter the measurement results. In smaller furnaces more attention should be given to the exact position.

It should be noted, that in very specific occasions it is possible for the total heat flux to be lower than the radiative heat flux. This occurs when the probe is of higher temperature than its environment. The total heat flux meter pellet will then heat the surrounding gas by convection. The convection part of the total heat flux will thus have a negative contribution.

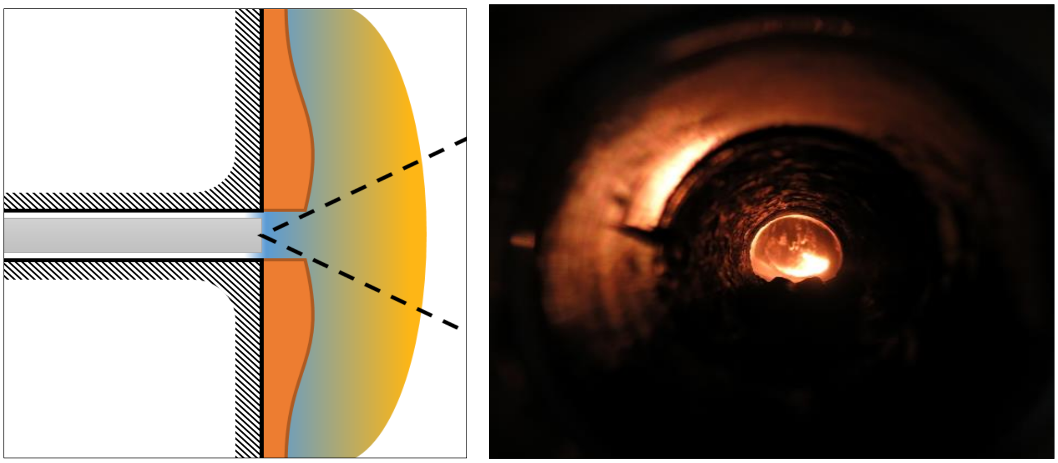

Figure 9 Port obstruction

2.5 Data recovery equipment

Measurements acquired by the thermocouples are collected by the laptop using the Agilent 34970A datalogger and corresponding software called *free Benchlink datalogger software*.

The Agilent 34970A datalogger is able to measure and convert 11 different input signals in total. Different signals relevant for measurements in CUIDEN are listed as: temperature with thermocouples; dc volts; 105 Ohm-wire resistance; dc current [8]. Table 5 provides a list of all different input signals for the pyrometer and heat transfer probes. The data logger is able to communicate with the laptop using voltage signals. The free Benchmark data logger software can be used to obtain the temperatures, since Thermocouple polynomials to convert voltage into temperature are already preprogramed. Calculations for heat fluxes are too complex for the Benchmark data logger software and have to be performed in post processing using Excel. Further specifications are frequency acquisition is two seconds for all signals and values are recorded in ".csv" files which can be processed in Microsoft Excel. The 'continuous' recording allows for the use of a statistical analysis, where average and deviation of the measured values are calculated in a time window between 'start time' and 'end time'.

Signal	tag	signal	measure unit	measure range
Radiative heat flux	RHF	mV	mV	0-5000
Temp. thermocouple 1	THF1	tc K	°C	0-1250
Temp. thermocouple 2	THF2	tc K	°C	0-1250
Gastemp. pyrometer	TPYRO	tc S	°C	0-1750
Watertemp. pyrometer	TWPYRO	tc K	°C	0-1250

Table 5, list of signals

3 Calibration of ellipsoidal radiometer and total heat flow meter

Signals for both the ellipsoidal radiometer and total heat flow meter are in millivolts and have to be converted into heat flows. Standard IFRF policy is to do this by calibration. Subjects included in this chapter are a description about the black body furnace, the procedure for calibration, the calibration results, discussion and recommendations. All results can also be found in [Source], which is an extended study about the calibration procedure including probes from 3 different companies and calibration results over the last 3 years.

3.1 Black body furnace

The calibration is performed using a small black body furnace located in the IFRF workplace. Figure 11 shows a schematic overview of the black body furnace, Figure 10 shows the furnace during operation. Some characteristics: maximum current 94 A, voltage 220 V and maximum temperature 1600 °C [1].

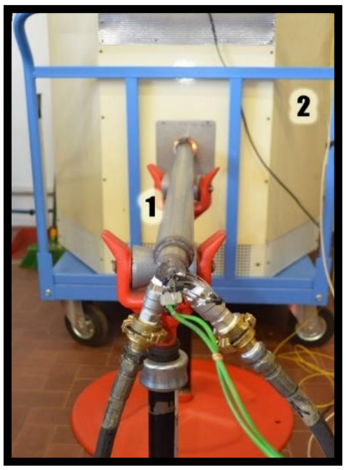

Figure 10, black body furnace

No.	*Part type*
1	Ellipsoidal radiometer
2	Black body furnace
3	Thermocouple inside black body sphere
4	Thermocouple outside black body sphere
5	Heating element
6	Black body sphere

Table 6, list of all components with corresponding numbers

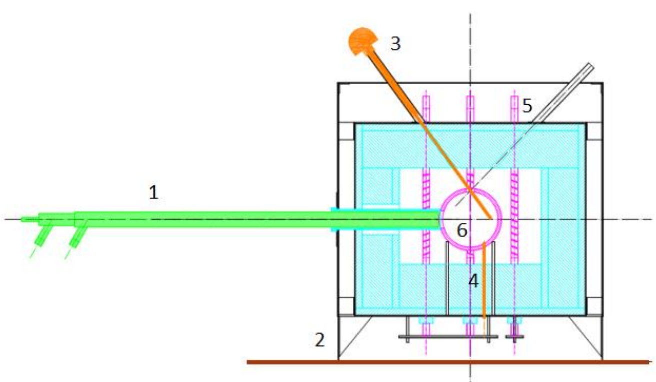

Figure 11, schematic overview black body furnace [9]

For the heating the black body sphere the furnace uses six silicon carbide electrical heaters which are placed in the inner furnace volume. The black body sphere is a silicon carbide 180mm diameter empty sphere, with a wall thickness of 10mm and a 50mm diameter hole to insert instruments to calibrate. Regulation of the black body furnace happens by the external thermocouple which is very close to the surface of the hollow sphere. A second thermocouple is placed into the black body sphere and measures the real temperature of the radiative source. So when the probe is inserted it is easy to calibrate for this known temperature. To receive the radiation flux from the inner black body surface the RHF and the THF meters position is 5 mm from to the black body. A 60 x 50 mm ceramic shield protects the probes from electrical heaters radiation.

Additional data recovery equipment for calibration is similar to the data recovery equipment for the measurement campaign, including Agilent 34970A data logger and free Benchlink data logger software, a laptop and both heat flux probes.

3.2 Procedure calibration

Using the black body furnace calibrations for the Radiative heat flux meter and Total heat flux meter were performed. This is done by measuring signals from both probes at different set point temperatures. A measurement is taken at a set point temperature when a steady state is reached. After the measurement the calibration proceeds to the next set point with a rate of 12°C/min. In order to obtain the best calibration, the set points are approached from higher and lower temperatures. This is accomplished by measuring the set points once in increasing order and once in decreasing order of temperature. Operation of the probes during the measurement campaign resulted in small variations in the performance. Hence both probes are calibrated both before and after the measurement campaign and results averaged. After each calibration case the results are processed to obtain both the average and deviation for the different signals. The time range for the obtained signal values in each set point temperature is 15 minutes, for which the black body furnace operates in steady state condition.

3.2.1 Calibration radiative heat flux meter

For the radiative heat flux meter there are 2 signals, both the radiative heat flux signal RHF_{out} (mV) and furnace temperature T_{BB} (°C). The total heat flux between the radiative heat flux meter and black body furnace can be calculated according to 3-1.

$$\dot{Q}_{rad} = \sigma\epsilon(T_{BB}^4 - T_{RM}^4) + h(T_{BB} - \mathrm{T}_{RM}), \qquad [W/m^2K]$$

3-1

$\dot{Q}_{rad}$	= heat flux to RHF meter
σ	= Stefan Boltzmann constant
ϵ	= total emissivity of the surface
T_{BB}	= temperature in the black body furnace
T_{RM}	= temperature of the RHF meter
h	= Coefficient of convective heat transfer

Which is the sum of the natural convection and radiation. The policy of IFRF is to leave out the contribution by natural convection and assume that the T_{RM} is much smaller than the T_{BB}, in addition, emissivity is assumed to be equal to the emissivity of an ideal black body. The motivation is that the resulting uncertainty of these assumption will be within the final uncertainty of calibration, and will therefore not harm the results. Hence the radiative heat flux between the radiative heat flux meter and black body furnace can be calculated according to 3-2.

$$\dot{Q}_{rad} = \sigma\epsilon T_{BB}^4, \qquad [W/m^2]$$

3-2

Since the radiative heat flux is known for a given furnace temperature, it is possible to couple the radiative heat flux to the radiative heat flux signal.

3.2.2 Calibration total heat flux meter

For the total heat flux meter there are 3 signals, the furnace temperature T_{BB} (°C), the temperature of Thermocouple 1 T_{tc1} (°C) and Thermocouple 2 T_{tc2} (°C). The total heat flux is assumed to be calculated similar to the radiative heat flux. In addition, a proportional constant k_{THF} as function of the temperature is defined as 3-3.

$$k_{THF} = \frac{Q_{tot}}{\Delta T} = \frac{\epsilon \sigma T_{BB}^4}{T_{tc1} - T_{tc2}}, \qquad [W/m^2 K]$$

3-3

Since the furnace temperature is known for a given furnace set point temperature, it is possible to couple the proportional constant to the average temperature between thermocouple 1 and 2.

3.2.3 Calibration signal errors

All of the signals contain errors which are known values or can be calculated, an overview of all the signal errors is shown in Table 7. By implementing these errors in the collected data it is possible to obtain the combined error for the different calibration parameters. Using Excel this is done by creating worst case scenarios for each calibration parameter. All worst case scenarios are plotted in a scatterplot and the corresponding linear regression parameters are used to couple signals to the heat flux.

For error calculation the traditional method of error propagation is used, according to 3-4.

$$\Delta y = \sqrt{\left|\frac{\partial y}{\partial x_1}\right|^2 \Delta x_1 + \left|\frac{\partial y}{\partial x_2}\right|^2 \Delta x_2 + \cdots} \ , \qquad y = f(x_1, x_2, \dots)$$

3-4

Which can be explained as the change of the function as result of the change of its variables.

Error sources	RHF	THF	Value	Unit	Description
Voltmeter	X		0.07	mV	--------
Furnace temperature	X	X	±2.5 between −40 °C and 333 °C, ±0.0075×T between 333 °C and 1200 °C	°C	Error related to performance thermocouple
TC 1		X	Idem	°C	Idem
TC 2		X	Idem	°C	Idem
Deviation all signals	X	X	-	-	Deviation from average value over a time range

Table 7, list of signal errors

3.3 Calibration results

This section shows all the results for calibration of the IFRF heat flux probes. The IFRF calibration results are based on the combination of all calibration procedures. All results consist of regression lines for calibration of the heat flux meters as well as error predictions, shown in Figure 12 and Figure 13 . Error margins are calculated with the errors of the different coefficients making up the regression lines. In some cases this will produce unrealistic errors, in these cases the average error of the regression line is used.

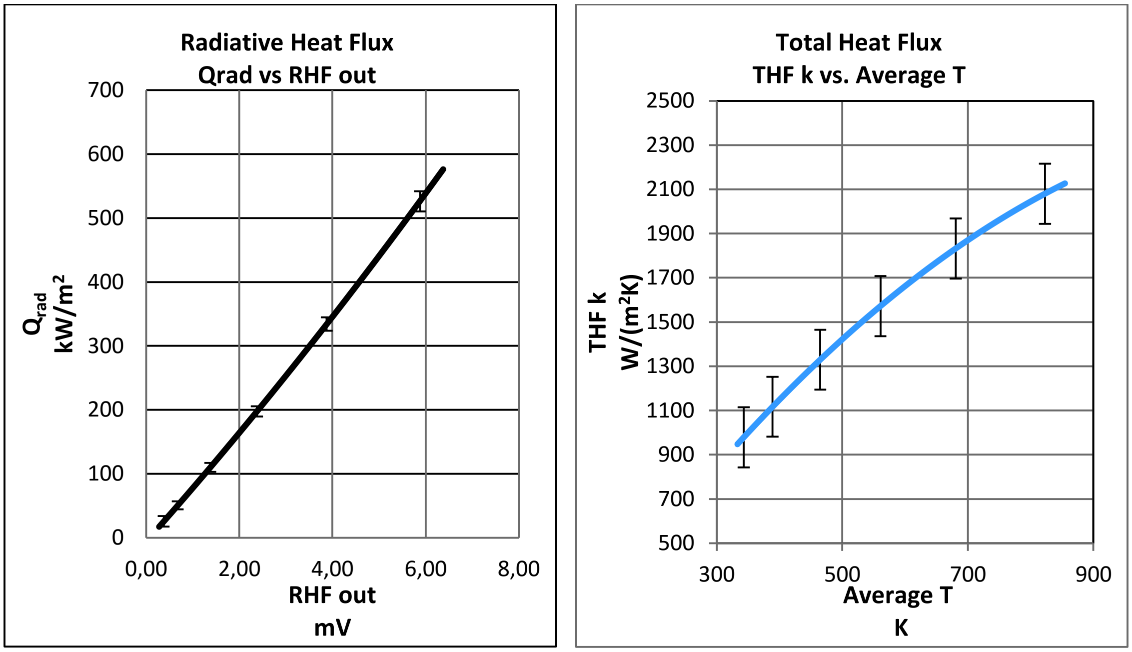

Figure 12 a), b), calibration results for radiative heat fluw meter (left) and total heat flux meter (right)

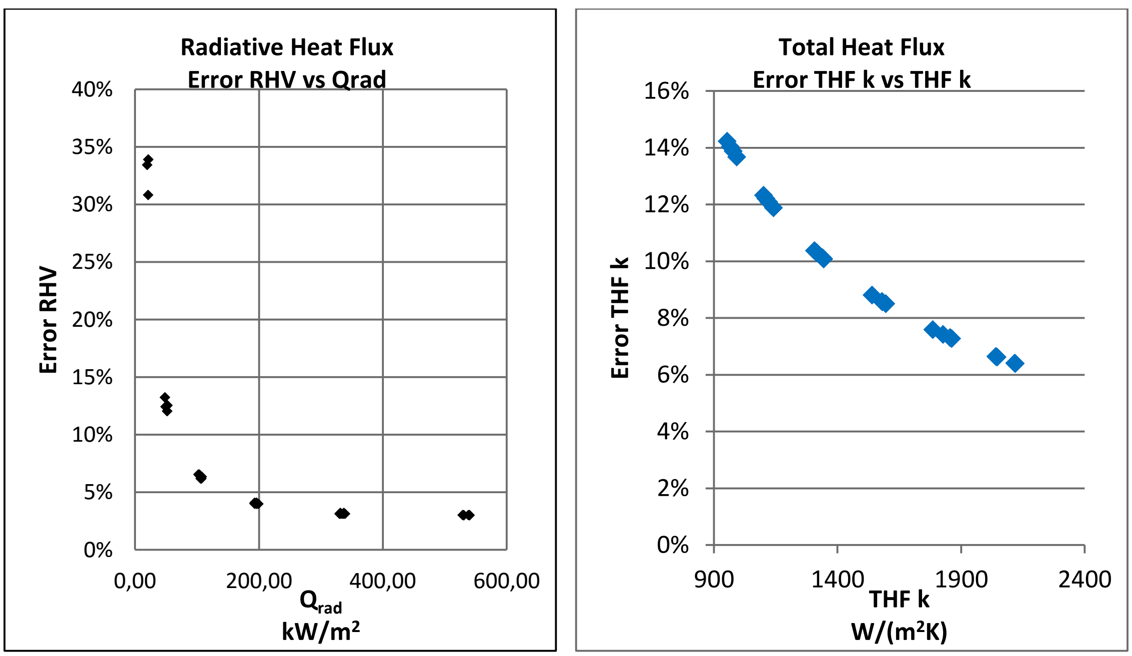

Figure 13 a), b) error behavior for radiative heat fluw meter (left) and total heat flux meter (right)

The figures can be used to make some observations about the performance of both heat flux meters. Both heat flux meters perform better within the higher temperature range 900-1500°*C.* The radiative heat flux meter error shows an asymptotic behavior converging towards 3-4%. The average error is about 4%, excluding values for 500-700°*C.* The total heat flux has an average error of 8%, with a fixed absolute error of 136 W/m^{2}K. Based on observation of the behavior of the signals it was found that the typical response time of the total heat flux meter is in the order of 10 minutes, which is related to the use of stainless steel plugs. Similarly the typical response time of the radiative heat flux meter is in the order of 2 minutes.

3.4 Discussion results

When looking at the results for the total heat flux meters, it can be seen that the error values are relatively high compared to the radiative heat flux. This means that behavior of the total heat flux meters differs during calibration for the different cases. Figure 14 compares results from the latest calibration method for both increase and decrease in set point temperature, before and after the measurement campaign. In addition, a difference in percentage between the regression lines is plotted in each chart. The difference is calculated by dividing the absolute difference by the average of both regression lines.

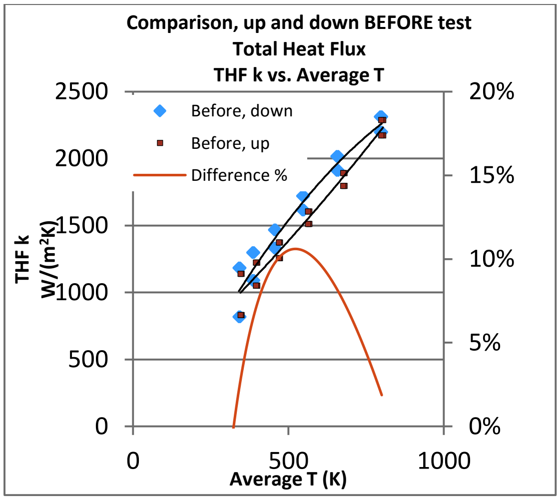

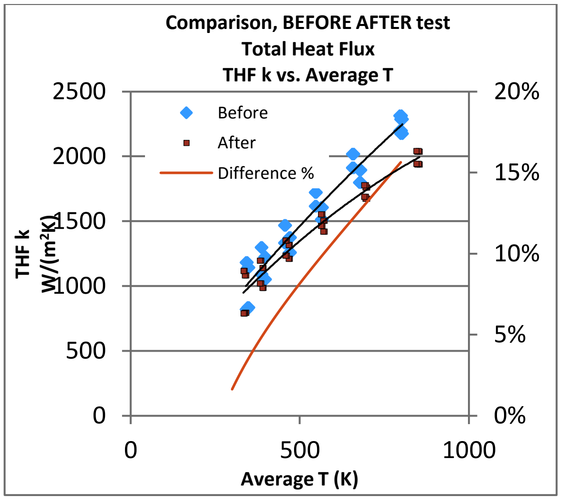

Figure 14 a), b), comparison of the different calibration cases, total heat flux meter

It can be seen that differences can reach values up to 12 % for the comparison between increase and decrease in set point temperature, and values up to 17% for comparison before and after the measurement campaign.

The difference between before and after the measurement campaign can be explained by the change in performance when operating in industrial environment with slug and dust settlement, plugging of the air channels causes additional conductive heat transfer in radial direction. Since the amount of heat entering the total heat flux meter stays constant this means less conductive heat transfer in axial direction. The decrease in axial heat transfer leads to a lower temperature at TC2. The temperature at TC1, being close to the surface, does not change much. Therefore a bigger temperature difference is measured. This will be observed as a decreased proportionality constant for the same average temperature, as can be seen in Figure 14 b). To limit the decrease in performance the total heat flux probe is regularly cleaned by removal of the ash from the insulation channels.

The difference between the cases of increase and decrease in set point temperature can be tracked back to the results of the different output signals T_{BB} (°*C*), T_{tc1} (°*C*) and T_{tc2} (°*C*). Figure 15 is used as example for the behavior of the thermocouple signals, results for the before measurement case are used.

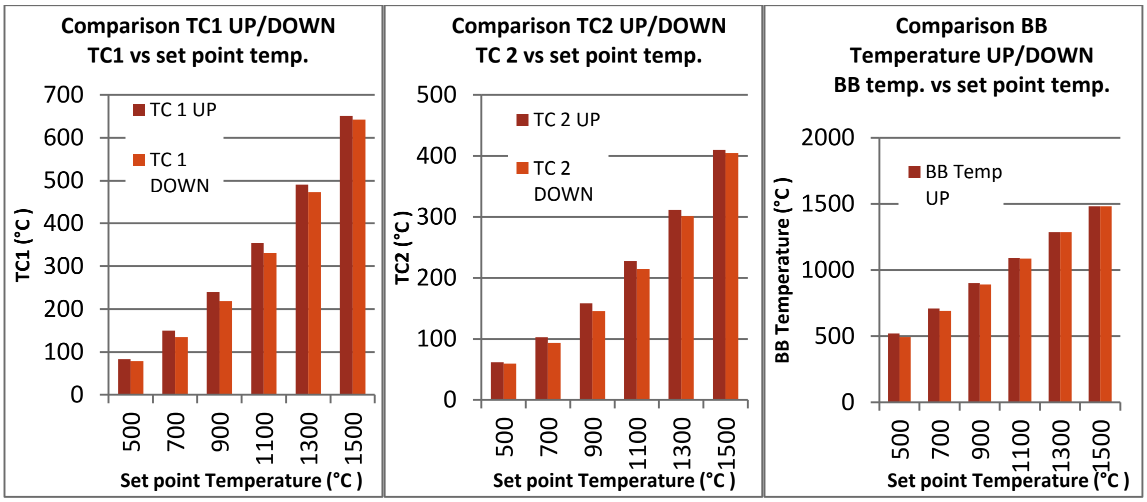

Figure 15 a), b), c) Comparison thermocouple signals for increase and decrease in set point temperature

Thermocouple output signals show higher values for an increase in set point temperature than a decrease in set point temperature. This dependency of the output signal to the increase or decrease of the black body furnace temperature signifies the need for analysis of the black body furnace and possibly improve the total heat flux meter. To explain the difference in temperature output signals Figure 16 is used. Figure 16 shows the behavior of the different thermocouples when the black body furnace reaches a new set point temperature for both an increase and decrease in set point temperature. The set point temperature of the black body furnace is 1100 °*C.*

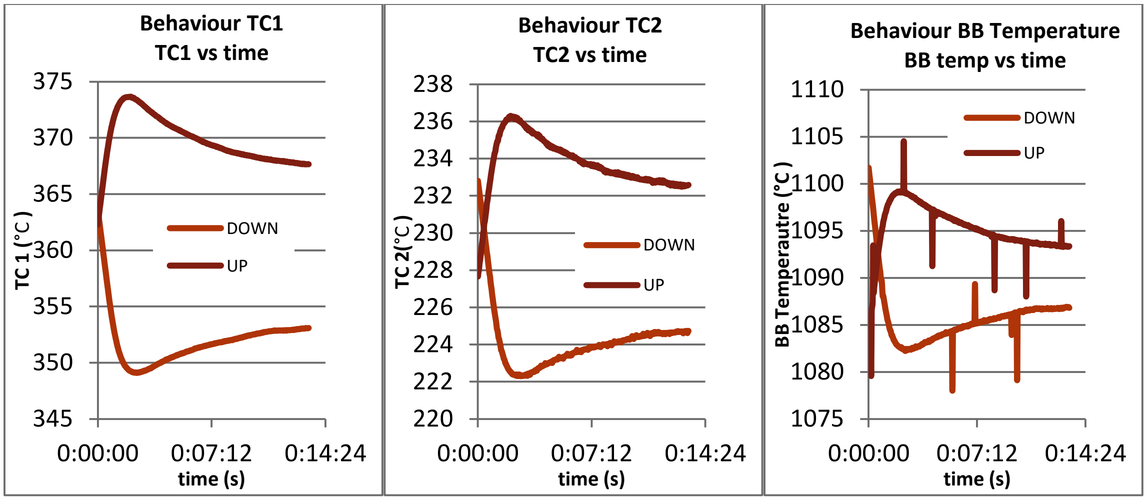

Figure 16 a), b), c), behavior thermocouple signals over time when reaching new set point temperature, both increase and decrease in set point temperature

The black body furnace uses a temperature regulator with a feedback signal. The feedback signal is given by a thermocouple positioned just outside the black body. When increasing the temperature of the furnace, the electrical heating elements will turn off if the feedback thermocouple reaches the set point temperature. However the heat produced by the electrical elements is delayed to the inside of the black body by surrounding air and material of the black body. This results in an overshoot of the temperature and a settling temperature inside the black body different than the specified set point. The steady state condition is typically reached in about 15 minutes.

The behavior of the temperature inside the black body sphere is asymptotic in nature. This means that over time the temperature will converge to a certain value. However, between heating and cooling of the blackbody furnace the eventual convergence value for the temperature differs. The reason for this is not known. But the consequence is different calibration results for an increase and decrease in set point temperature. To decrease the temperature difference, standard procedure is to wait 10-15 minutes before starting the calibration measurements in the set point. However, in order to fully prevent the temperature difference, redesign of the black body furnace is required.

A similar comparison was also performed for the radiative heat flux meter. But due to the active nitrogen injection the difference in performance before and after the measurement campaign were relatively small and not worth mentioning.

3.5 Conclusions calibration

The IFRF radiative heat flux meter error shows an asymptotic behavior converging towards 3-4%. The average error is about 4%, excluding values for 500-700*°C.* The total heat flux has an average error of 8%. With a fixed absolute error of 136 W/m^2K.

During the measurement campaign in CUIDEN, the total heat flux meter performance was influenced due to plugging of the channels. The changes in performance for the radiative heat flux meter were relatively small due to active injection of nitrogen.

The differences in total heat flux calibration results encountered during an increase and decrease in set point temperature can be tracked back to a difference in the thermocouple signal values for increase and decrease in set point temperature.

After reaching the set point temperature, the black body furnace needs a certain amount of time to reach steady state conditions.

3.6 Recommendations calibration

In order to obtain better results for the heat flux probes in future measurement campaigns a number of recommendations are presented.

The total heat flux meter is calibrated by measuring the temperature difference between the two thermocouples. One of the shortcomings of the total heat flux design is that both thermocouples change during calibration. It would be better to keep one of the thermocouples more or less constant during calibration, reducing the amount of uncertainties by one. However, the current design is unable to disperse the thermal energy by conduction fast enough, leading to thermal energy build up at the cold side of the total heat flux meter, this effect is shown in Figure 15 b). Therefore it is advised to redesign the total heat flux meter for more efficient energy dispersion.

One of the biggest reductions in the performance of the total heat flux meters is the build-up of ash and soot in the insulation channels. Leading to conductive heat transfer in radial direction. Since there is no reason to expose the insulation channels to the outside environment it is advised to introduce a modification in the design to enclose the insulation channels. But still leave the total heat flux meter core free to move in axial direction to compensate for thermal expansion.

Some assumptions have been introduced for the calculation of the total heat transfer in the black body furnace. Simply assuming the temperature of the probe and the convective heat transfer to be negligible small, as well as an emissivity similar to that of an ideal black body. The motivation is that the additional uncertainties of these assumptions are well within the total uncertainty results found during calibration, however this should be verified.

4 Experimental campaign measurement results and discussion

After calibration of both heat flux probes it is possible to implement the processed average and standard deviation of the signals in order to obtain heat transfer values. Subjects included in this chapter are the processed data from the ellipsoidal radiometer, total heat flow meter and pyrometer. In addition, observations, conclusions and discussion of the different cases.

4.1 Results heat flux

The heat fluxes for the different combustion modes are shown in **Error! Reference source not found.**, including the radiative heat flux, total heat flux and convective heat flux versus the distance from the burner outlet to the measurement port. Assuming no additional contributions to the total heat flux, the convective heat flux can simply be calculated by subtracting the radiative heat flux from the total heat flux. The results can help study the potential heat transfer to the heat exchangers positioned in the walls of the furnace.

It can be seen that all modes have dominant contributions of the radiation to the total heat transfer, with smaller contributions by the convective heat transfer. However the ratio radiation/convection differs per combustion mode. For example values for the S2-O17 are respectively smaller, leading to bigger values for the convective heat transfer. This could indicate an especially active flow with high convective heat transfer. It can also be seen that total heat flux values for the S2-O1 are significantly smaller close to the burner. Although radiative heat flux is not measured for this point it possible to couple this to the relative low temperature values found in port 7, close to the burner Figure 18 a). It should be mentioned that many uncertainties were introduced when measuring the heat transfer along the walls of the furnace. Especially due to ash settlement on the surface of the probes or the furnace walls. In some measurements the probes were unable to reach the inside of the furnace, leading to measurements in the thick layer of ash. Therefore some of the measurement have been repeated with additional insertion depth. In addition, regular cleaning ensured that the performance would be maintained.

4.2 Results pyrometer

Obtaining the average temperature and standard deviation for the suction pyrometer proved troubling. Therefore IFRF developed a method to verify the insertion depth of the probe. The next section will contain a description about the processing method for temperature before providing results for temperature measurements.

4.2.1 Processing method Temperature

As stated before, the values for temperature in a measurement point were recorded in a time frame and used to calculate both the average temperature and standard deviation. However during the measurement campaign miscommunication caused errors in the time frame and processed data, hence shifts in the timeframe were required. Since the Temperature values for different insertion depth cannot be distinguished based on the TPYRO signal, IFRF uses values obtained from water temperature pyrometer (TWPYRO) as well. Figure 17 shows a temperature vs time plot for both TPYRO and TWPYRO. Measurement time frames for temperature are specified by yellow lines plotted on top of the TPYRO and can be shifted back and forth depending on the most stable temperature vs time frame within the defined insertion depth.

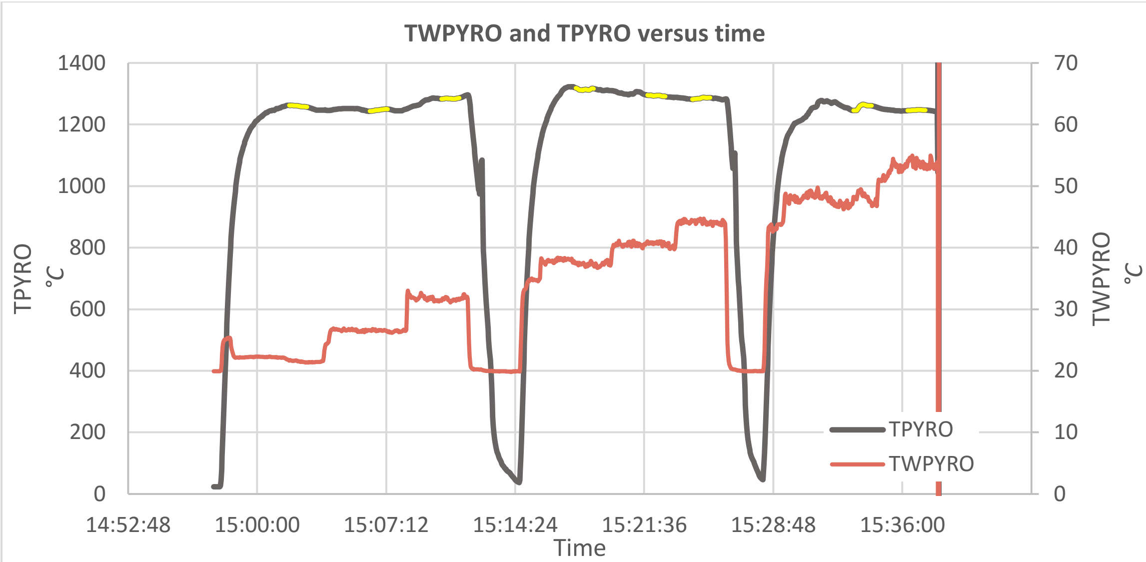

Figure 17, behavior Pyrometer water temperature and Pyrometer temperature

All temperature data are processed using the method described above. In the next section a selection of charts will be shown, giving a representation of the results obtained for the temperature.

4.2.2 Results Temperature

In comparison of the different measurements, emphasize is on port 6 and 7 as these help study the properties of the flame. Port 7 being close to the burner shows an early stage of the combustion process while port 6, farther away from the burner, shows a more developed situation. Because the heat exchanges in the furnace are positioned behind port 32 temperatures results for the corresponding port help study the heat extraction.

Error! Reference source not found. shows temperature measurements taken from port 6 and 7 espectively, the position of the burner is specified along the boiler axis. For the air case temperatures are higher close to the burner, which indicates a flame closer to the burner. It can also be seen that after the peak temperature is reached, temperature decrease occurs by distribution of the heat and possibly secondary endothermic reactions for intermediate species. In oxy mode, S2-O17, more or less the same behavior can be seen as the air case. In the oxy mode, S2-O1, temperatures close to the burner are very low. This might indicate a flame positioned further away from the burner. In all cases lower temperatures are observed close to the walls of the furnace. One of the reasons is that all furnaces operate at under pressure for safety reasons, since the probes do not seal the opening of the port completely this will lead to air in leakage in the furnace. However, it is impossible to verify these observations without the support of the chemical species results, which are discussed in [4].

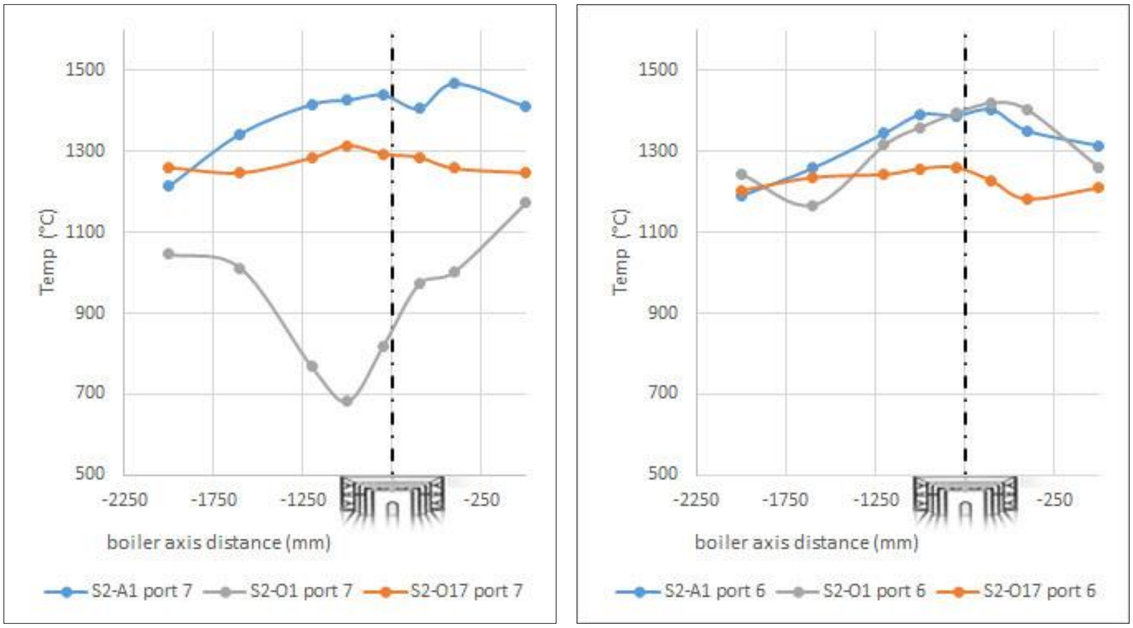

Figure 18 a), b), Temperature profiles in port 7 (left) and port 6 (right)

Error! Reference source not found. shows the temperature profile for port 32. Based on the results of Figure 18 and **Error! Reference source not found.** it can be observed that all temperatures of the Oxy modes are more or less the same to the Air mode. This indicates that the introduction of the flue gas recirculation with the correct recycle ratio was indeed successful, since no additional thermal strain and NO_x formation will be introduced to the furnace.

Since the heat exchangers are positioned behind port 32, it is possible to make an estimation about the heat extraction by the heat exchangers. In order to do this, some characteristics of the furnace outlet also have to be known.

In order to calculate the heat extraction a list of characteristics of the furnace is provided in **Error! Reference source not found.**, including composition of the flow, average temperatures and mass flow.

The heat extraction is calculated using the mass and energy balance over the furnace stack, according to 4-1.

$$h_{in}\dot{m} = h_{out}\dot{m} + \dot{Q}_{extraction}, \qquad [kW] \tag{4-1}$$

h	= specific enthalpy
m	= mass flow of the flue gas inside the furnace
$Q_{extraction}$	= heat extraction between port 32 and exit furnace

Assuming kinetic and potential energy are negligible small and no additional mass is added by air in leakage. The combined enthalpy of the flue gas can be calculated according to 4-2.

$$h_{FG} = \left(1 - x_{H_2O}^{w.b.}\right)\left(x_{N_2}^{d.b.} h_{N2} + x_{O_2}^{d.b.} h_{O2} + x_{CO_2}^{d.b.} h_{CO2}\right) + x_{H_2O}^{w.b.} h_{H2O}) \ [kJ/kg]$$

4-2

However, since all the compositions are given in the volume fraction these first have to be converted into mass fraction. This is done using the following relation between mass fraction and volume fraction, 4-3, 4-4.

$$x_i = \frac{\rho_i}{\rho} y_i$$

4-3

$$\rho = \left(1 - x_{H_2O}^{w.b.}\right)\left(x_{N_2}^{d.b.} \rho_{N2} + x_{O_2}^{d.b.} \rho_{O2} + x_{CO_2}^{d.b.} \rho_{CO2}\right) + x_{H_2O}^{w.b.} \rho_{H2O}) \ [kg/m^3]$$

4-4

y = volume fraction of the species
x = mass fraction of the species
ρ = density

Values for the enthalpy and density for the different species are extracted from a real fluids database provided by EES. However, due to the higher temperatures in the furnace, it proves troublesome to find the enthalpy and density for some of the species. In these cases ideal gas was assumed. The results for the energy extraction for all cases are shown in Figure 19. In addition the amount of energy fed to the furnace by coal is calculated to give some indication about the percentage leaving through the heat exchangers and walls after port 36. A big part of the thermal energy is already transferred though the walls of the furnace.

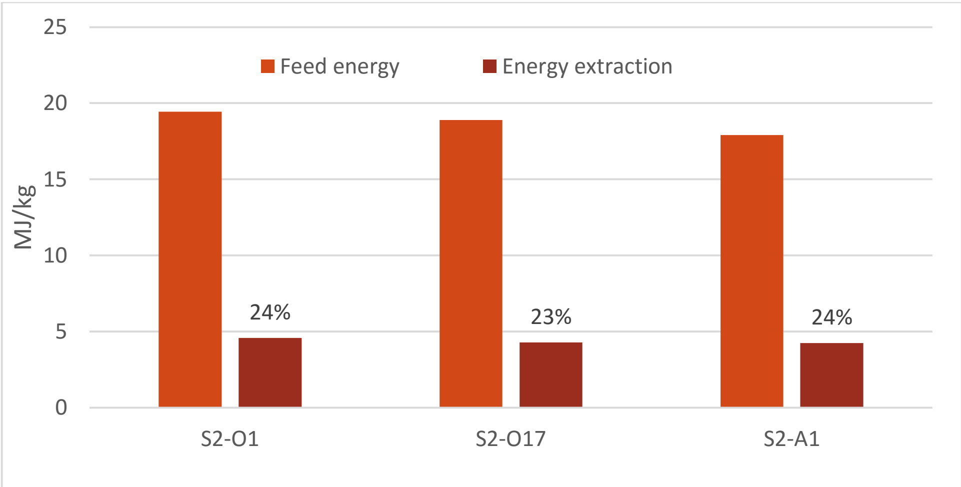

Figure 19, Energy balance between port 32 and the furnace outlet

Figure 19 indicates that the heat extraction as percentage of the feed energy is more or less the same for the different modes. It is not known if this is coincidence or a direct result of the regulation of the amount of working medium flowing through the heat exchanger. In addition, it can also be seen that biggest part of the heat is already withdrawn from the furnace before the flue gas arrives at port 32, even though a part of the heat energy also remains in the flue gas after leaving the furnace.

4.3 Conclusions measurement results

The introduction of the flue gas recirculation leads to reduction in the overall temperature inside the furnace. In all oxy modes this was successfully implemented by choosing the correct recycle ratio, as can be seen by the more or less the same temperature results for the different modes.

The biggest part of the overall heat extraction occurs before the flue gas arrives at port 32. Mainly by heat exchangers located in the walls of the furnace.

4.4 Discussion measurement results

All results obtained during the measurement campaign contain a predetermined uncertainty, either calculated by calibration or analytically. However, operation in an industrial environment where situations are harder to control can also lead to additional uncertainties. Since the data were not verified by repeating the measurements not much can be said about these uncertainties, except that they do exist.

One of these uncertainties is the unstable operation of the furnace. The furnace operated with 4 burners, which interact and show different behaviour in their performance. The ignition of the coal was observed by infrared cameras placed inside the furnace. When the camera had negative readings standard procedure was to inject additional methane to boost the ignition of coal. All in all the CUIDEN combustion unit is very complex and there are a lot of unknowns. So even though the different modes have fixed operation conditions, these conditions where far from fixed during operation.

5 References

1. G. Coraggio, M.F., *IFK and TUM Radiative Heat Flux and Total Heat Flux calibration procedure*, April 2015, International Flame Research Foundation: Livorno.
2. R. Diego (CIUDEN), M.F., G. Coraggio (IFRF), *Systematic oxyfiring at 20MW*, 2014, RELCOM Partners and European Commission.
3. Braud, J.C.a.Y., *Measurements in Flames*. Industrial Flames. Vol. 1. 1972: Edward Arnold. 228.
4. Geerligs, H., *Techniques for in-flame measurements*, 2015, University of Twente. p. 30.
5. IFRF, *Suction pyrometer user manual*.
6. Foundation, I.F.R., *Ellipsoidal radiometer user manual*.
7. Foundation, I.F.R., *Total Heat Flux Meter*.
8. Sun, J., et al., *Recycling of Waste Printed Circuit Boards by Microwave-Induced Pyrolysis and Featured Mechanical Processing.* Industrial & Engineering Chemistry Research, 2011. **50**(20): p. 11763-11769.
9. *Schematic overview of Black body furnace, property of IFRF*.